Research Article

Yanchao Qiao and Lijie Duan*

Curcumin-loaded polyvinyl butyral film with antibacterial activity

https://doi.org/10.1515/epoly-2020-0042
received October 30, 2019; accepted May 11, 2020

Abstract: Antibacterial materials have found widespread interest in different fields nowadays. In this study, curcumin (Cur) was incorporated into the polyvinyl butyral (PVB) matrix by dissolving in ethanol for improving the functional properties of a pure PVB film. We found that Cur was uniformly dispersed in the PVB matrix, which showed good compatibility. Moreover, the incorporation of Cur could also improve thermal stability, hydrophilicity, and mechanical property. The UV-vis spectra of the PVB–Cur film demonstrated that the film could block ultraviolet radiation. Subsequently, the antibacterial activity of the PVB–Cur film was measured by the colony-counting method against *S. aureus* and *E. coli*. The results showed that the PVB–Cur film exhibited good antibacterial activity. Therefore, the PVB–Cur film was considered as a promising material for food and medical packaging applications.

Keywords: curcumin, polyvinyl butyral, film, antibacterial activity

1 Introduction

In recent years, various films, especially the antimicrobial films, have been rapidly developed. Usually, antimicrobial materials such as silver nanoparticles (1), metal oxides (ZnO, CuO, TiO_2) (2), organic acids (benzoic acid, sorbates) (3), enzymes (lysozyme, glucose oxidase) (4), natural active compounds (essential oil, biopolymer, pomegranate-rind extract, and curcumin (Cur)) (5–7), antibiotics, triclosan, and other functional ingredients were incorporated into polymers (natural or synthetic) to fabricate antimicrobial films (8,9). Furthermore, some researchers prepared multifunctional composite materials with antibacterial activity and antioxidant activity (10,11).

Cur [1,7-bis(4-hydroxy-3-methoxyphenyl)-1,6-hepadiene-3,5-dione] is a kind of polyphenolic phytoconstituent found in the rhizomes of *Curcuma longa* (turmeric) with antibacterial, anti-inflammatory, anticancer, and antioxidant activities (12–14). Turmeric has been used as a spice and traditional natural herbal medicine for thousands of years (15,16). The Cur extracted from turmeric has reactive oxygen species scavenging ability to improve the wound healing process due to a large number of phenolic hydroxyl groups in the molecule chain (17). Clinical trials have shown that Cur was safe, even when applied to humans at high doses (12 g/day) (18).

In previous work, Liu et al. prepared Cur–chitosan (Cur–CH) blend films by the solution casting technique. The resulting blend films showed excellent tensile strength and antibacterial activity (19). Luo et al. prepared cellulose/Cur composite films using ionic liquid (1-allyl-3-methylimidazolium chloride (AmimCl)) as a solvent. The composite films containing Cur exhibited good mechanical properties, thermal stability and antibacterial activity, which could be applied in food packaging and medical fields (20). Moreover, Govindaraj et al. fabricated *C. longa* oil-loaded polyacrylonitrile (PAN) films by the facile solvent casting technique. Incorporation of *C. longa* oil into the PAN matrix increased the hydrophilicity of the films (21). Besides, Li et al. developed a methoxy poly(ethylene glycol)-*graft*-chitosan film loaded with Cur nanoformulation (Cur–MPEG–chitosan film). The in vivo wound healing test showed that the Cur–MPEG–chitosan film was effective in wound healing (22).

Polyvinyl butyral (PVB) is synthesized by the acetalization of polyvinyl alcohol (PVA) and butyraldehyde under acidic conditions. PVA is a polymer prepared from the polyvinyl acetate precursor; thus, a small portion of vinyl acetate units remain in the PVA (23). Therefore, PVB can be regarded as a ternary random polymer mainly composed of vinyl butyral and vinyl alcohol units and containing a small number of vinyl acetate units. PVB can be made into films

* **Corresponding author: Lijie Duan,** School of Chemistry and Life Science and Advanced Institute of Materials Science, Changchun University of Technology, Changchun 130012, People's Republic China, e-mail: duanlijie@ccut.edu.cn, tel: +86-431-85717352, fax: +86-431-85716465
Yanchao Qiao: School of Chemistry and Life Science and Advanced Institute of Materials Science, Changchun University of Technology, Changchun 130012, People's Republic China

with excellent mechanical property, optical clarity, biocompatibility, nontoxicity, and adhesive property (24,25).

In this investigation, we incorporated Cur into the PVB matrix using ethanol as solvent to fabricate Cur-loaded films (26–31). The films were characterized by Fourier transform infrared (FTIR) spectroscopy and UV-vis spectroscopy. The results indicated that the Cur was uniformly dispersed in the PVB matrix. In addition, the resultant PVB–Cur film exhibited thermal stability, high hydrophilicity, excellent mechanical strength, UV resistance, and antibacterial activity, which implied the potential applications in food packaging and medical fields.

2 Experimental

2.1 Materials

PVB (MW 40,000–70,000) and Cur (AR) were bought from Shanghai Macklin Biochemical Co., Ltd, China. Ethanol (AR) and sodium chloride (NaCl) (AR) were supplied by Beijing Chemical Works, China. Yeast extract (FMB Grade) was obtained from Shanghai Sangon Biotech Co., Ltd, China. Peptone (BR) was purchased from Beijing Aobox Biotechnology Co., Ltd, China. Agar powder (AR) was bought from Tianjin Guangfu Fine Chemical Research Institute, China. The species of bacteria were *Staphylococcus aureus* (*S. aureus*) (ATCC25923) and *Escherichia coli* (*E. coli*) (ATCC-25922), respectively.

2.2 Preparation of Cur-loaded PVB film

PVB films with Cur were prepared by a solution casting technique. Firstly, the PVB solution (6% w/v) was prepared by dissolving PVB in ethanol and the mixture was stirred using a magnetic stirrer hot plate (IKA, RT 15 S025, Germany) at 30°C with a rotor speed of 400 rpm. The transparent and homogeneous solution was obtained after being mixed for 90 min. Cur was subsequently added to the solution and continuously stirred for 30 min. The added content of Cur was 5% of the weight of PVB, which was determined through pre-experiments of tensile strength and antibacterial activity. The mixtures were ultrasonically treated at an ultrasonic power of 200 W and a frequency of 40 kHz for 10 min. The stable and homogeneous solution was cast onto the polyfluortetraethylene plate and then dried at 37°C to obtain films. The prepared composite films were defined as PVB–Cur films (Figure 1). For comparison, the pure PVB films were prepared by the same method.

2.3 FTIR analysis

The FTIR spectra of films were recorded on an iS50 FTIR spectrometer (ThermoFisher Nicolet, USA) with attenuated total reflection mode at room temperature, and the spectra of the films were scanned in the range of 500–4,000 cm^{-1} with a resolution of 4 cm^{-1}.

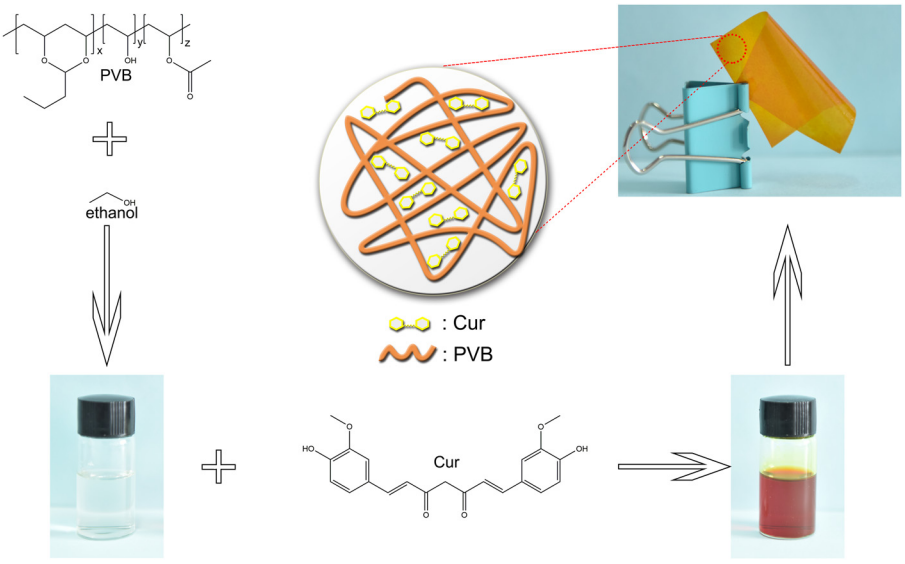

Figure 1: Schematic diagram of Cur-loaded PVB films.

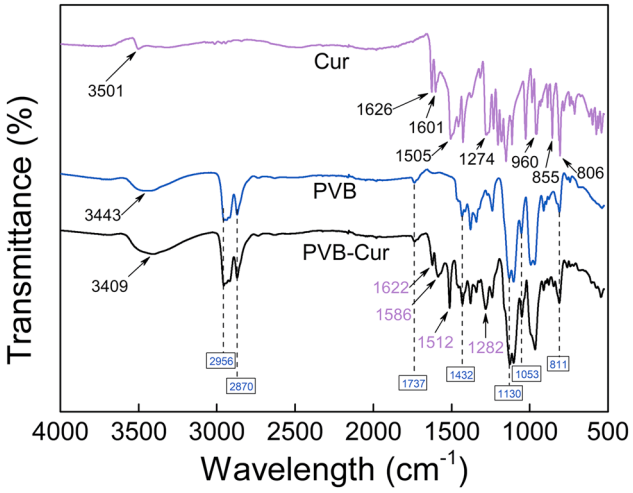

Figure 2: FTIR spectra of Cur, PVB, and PVB–Cur film.

2.4 Optical property

The ultraviolet and visible light barrier properties of PVB and PVB–Cur films were measured by using an ultraviolet-visible spectrophotometer (PerkinElmer, Lambda 25, USA). The film samples were cut into rectangular pieces (4 cm in length and 1 cm in width) and placed into the cuvette of spectrophotometer. The analyses were performed in triplicate. The transmittance of the film was measured in the wavelength range of 200–800 nm. Measurements were performed using air as a reference. The value of transparency is calculated, based on the transmittance of the film at 600 nm:

$$\text{Transparency value} = \log(T_{600}/d) \quad (1)$$

where T_{600} is the percentage transmittance (%) at 600 nm and d is the film thickness (mm).

2.5 Thermogravimetric analysis (TGA)

The thermal stability and degradation characteristics of the films were carried out on a thermogravimetric analyzer (METTLER TOLEDO, TGA 2, Switzerland). The sample weights for the test were 2–4 mg. The samples were heated up from 50°C to 600°C at a heating rate of 10°C/min under nitrogen atmosphere with a nominal gas flow rate of 50 mL/min.

2.6 Film thickness

The thickness of the films was determined by using a spiral micrometer (Ningbo Shiji Bosi Tools Co., Ltd, China). Six thickness values were randomly measured at different locations on each film and their average thickness values were calculated.

2.7 Mechanical property

The mechanical properties of PVB and PVB–Cur films were determined by using a tensile tester (SHIMADZU, AGS-X, Japan) with a 100 N load cell at a tensile rate of 5 mm/min. The initial grip separation was set at 35 mm and all samples were cut into strips (size of 5 mm width × 60 mm height). All the determinations were performed at room temperature of 25°C and were made in triplicate. The values of tensile strength and elongation at break were directly determined from the stress–strain curves (32).

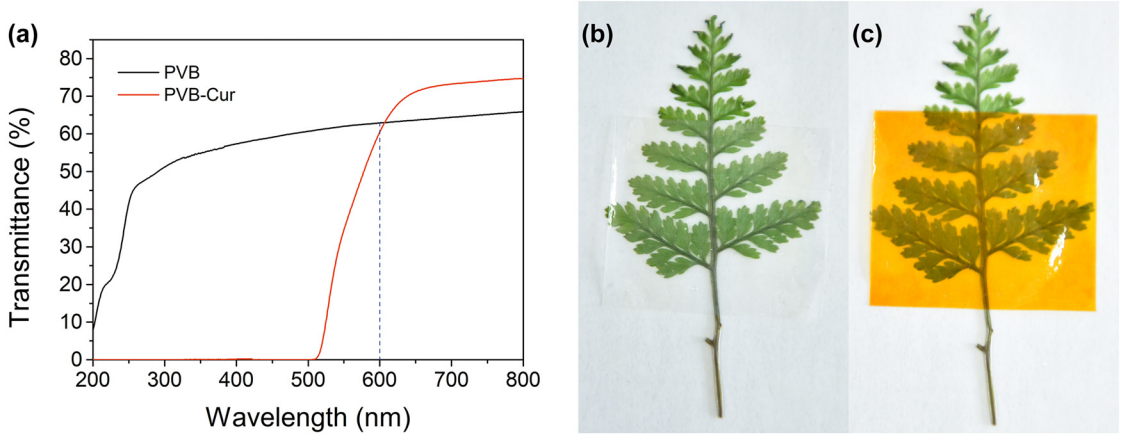

Figure 3: Light transmittance characteristics of PVB and PVB–Cur films. (a) PVB film under visible light and (b) PVB–Cur film under visible light (c).

2.8 Contact angle measurement

The water contact angle of the films was determined using a contact angle measurement instrument (HARKE-SPCA, Beijing, China). The samples (20 mm × 60 mm) were fixed to the glass substrate and their wettability was evaluated by a sessile drop method. A droplet (10 µL) of deionized water was placed on the film surface using a micro-syringe. The side-view images of the water droplets were recorded. The contact angles were measured. All measurements were performed at room temperature. The contact angle was measured at five random sites and then the average angle was taken.

2.9 Antibacterial activity assay

The antibacterial activity of the films was evaluated by the colony-counting method. Colony forming unit (CFU) assay was performed on two bacteria of *S. aureus* (ATCC25923) and *E. coli* (ATCC25922) isolates to determine the antimicrobial activity of the PVB–Cur film. A suspension of 108 bacteria was incubated with 1.0 mL of Luria–Bertani (LB) liquid culture medium containing PVB–Cur film (5.0 mg mL^{-1}), and compared to the untreated control, PVB film (5.0 mg mL^{-1}), free Cur (5.0 mg mL^{-1}, turbid liquid) groups. Tubes were incubated at 37°C for 4 h using a tube rotator to ensure a uniform distribution. After incubation, suspensions were serially diluted in phosphate buffer solution, plated onto tryptic soy agar, and incubated for 24 h at 37°C under aerobic conditions. Individual colonies were counted and the number of CFUs was tabulated.

3 Results and discussion

3.1 Chemical structure

The FTIR spectra of Cur (powders), PVB and PVB–Cur films are presented in Figure 2. In the spectrum of Cur, the peak at 3,501 cm^{-1} corresponded to the phenolic –OH stretching vibration. The absorption peak at 1,626 cm^{-1} was attributed to C=O stretching. The peaks at 1,601 and 1,505 cm^{-1} corresponded to C=C stretching in the benzene ring (33). The bands at 1,274 cm^{-1} corresponded to C–O of enol. Additionally, the bands in the region of 960–806 cm^{-1} belonged to C–H out-of-plane bending and aromatic stretching. PVB showed an absorption band at 3,443 cm^{-1} due to the –OH stretching, corresponding to the hydrophilic hydroxyl group in PVB. The peaks at 2,955 and 2,870 cm^{-1} were attributed to the asymmetric and symmetric $-CH_2$ stretching, respectively. The peak presented at 1,737 cm^{-1} was attributed to the carbonyl group double bond (C=O). The peak at 811 cm^{-1} was related to the presence of acetal groups. The out-of-plane bending hydrogen bond to the carbonyl group was observed at 1,053 cm^{-1} (34). The peak at 1,130 cm^{-1} was related to the vibration of C–O–C, and the peak of 1,432 cm^{-1} was due to $-CH_2$ bending. The characteristic peaks of Cur and PVB were presented in the spectrum of PVB–Cur films. It should be noted that in the spectrum of PVB–Cur film, the –OH stretching vibration of PVB showed a low-shift from 3,443 to 3,409 cm^{-1}. In addition, the C=O stretching of Cur shifted from 1,626 to 1,622 cm^{-1}; meanwhile, the C=C stretching in benzene ring at 1,601 and 1,505 cm^{-1} was shifted to 1,586 and 1,512 cm^{-1}, respectively. These results demonstrated that the hydrogen bonding between PVB and Cur was generated in PVB–Cur films. In brief, PVB and Cur had been compounded together excellently.

3.2 UV-vis analysis

Figure 3a shows the light transmittance of PVB and PVB–Cur films. The transmittance of the PVB film reduced at 600–200 nm. Moreover, the transmittance value of the PVB–Cur film almost reduced to 0% in the wavelength range of less than 500 nm. As we have known, Cur belongs to the class of phenolic compounds which is rich in unsaturated bonds, thus facilitating the absorption of

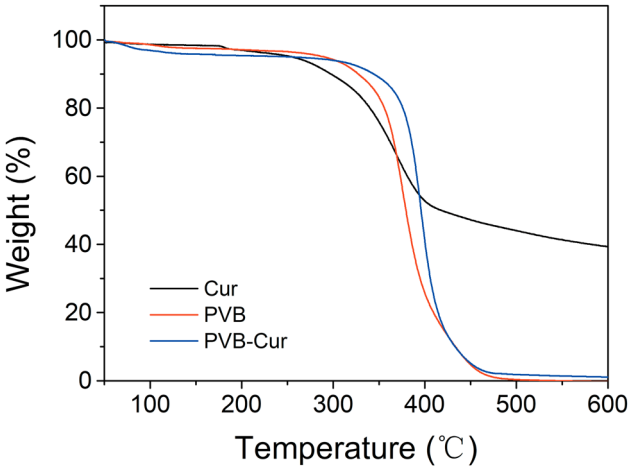

Figure 4: Thermal stability of PVB, Cur, and PVB–Cur films.

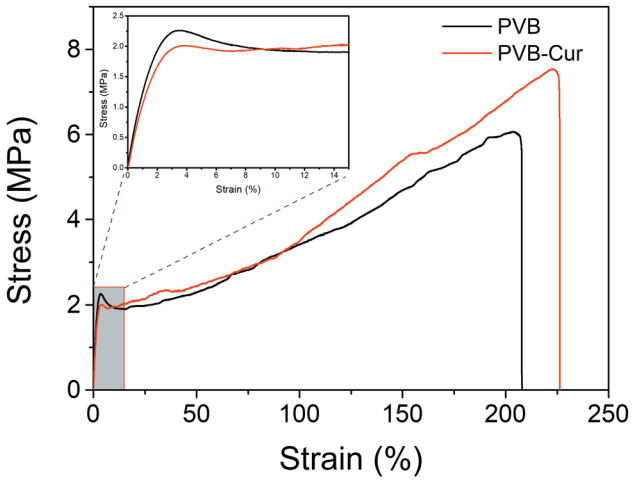

Figure 5: Strain–stress curves of PVB and PVB–Cur composite films.

ultraviolet radiation. Therefore, PVB–Cur film had superior UV-blocking properties than a PVB film. This film might effectively reduce the oxidative deterioration of food caused by light induction (35). Moreover, since UV light has a significant effect on the human wound, the PVB–Cur films with UV-blocking properties may be advantageous for inhibiting DNA rupture and dimerization of thymine molecules presented in the human wound. The transparency

Table 1: Thermal stability parameters for the PVB and PVB–Cur films.

Sample	T_{onset} (°C)	$T_{10\%}$ (°C)	T_{max} (°C)	Residue (%)
Cur	255	297	370	40
PVB	290	327	376	0
PVB–Cur	310	344	396	1

of the PVB–Cur film (2.94) and the PVB film (2.95) was almost equivalent at 600 nm, which indicated the good compatibility between Cur and PVB film matrix. Cur-loaded PVB films also had corresponding visualizations in Figure 3b and c.

3.3 Thermal stability

The thermal stability of PVB and PVB–Cur films was evaluated by the TGA. The primary thermograms of the films are shown in Figure 4 and the thermal properties are listed in Table 1. From the thermogram, it could be found that the residues of Cur powder and PVB–Cur film at 600°C were 40% and 1%, respectively, and the pure PVB film was completely degraded. The residue of Cur should be attributed

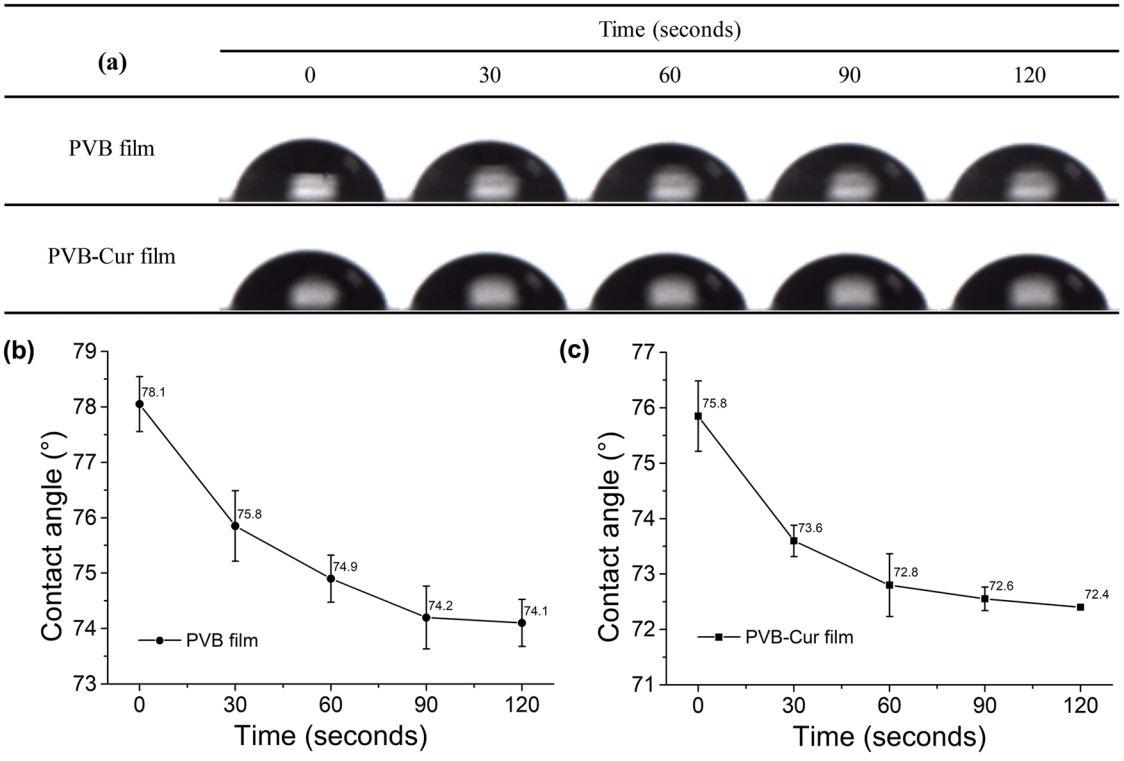

Figure 6: (a) Contact angle pictures and (b and c) contact angle values of water droplets on the surface of PVB and PVB–Cur films at different times.

to the presence of the phenyl rings. The initial weight loss temperatures (T_{onset}) of Cur powder, PVB film, and PVB–Cur film were 255°C, 290°C, and 310°C, respectively. Their maximum decomposition rates (T_{max}) were recorded at 370°C, 376°C, and 396°C, respectively. The $T_{10\%}$ ($T_{10\%}$ is the temperature of degradation at 10 wt% loss) values of PVB film and PVB–Cur film were 327°C and 344°C, respectively. The PVB–Cur film showed higher $T_{10\%}$, and T_{onset} and T_{max} values relative to the neat PVB film. This indicated that the degradation was shifted to a higher temperature, and the thermal stability of the composite film was improved by adding Cur to the PVB polymer matrix. The improved thermal stability observed for the PVB–Cur films might be attributed to the good dispersion of Cur in the polymer matrix. Meanwhile, these results indicated the potential of the PVB–Cur films applied at high temperatures.

3.4 Mechanical property

Figure 5 shows the tensile stress–strain curves of the PVB and PVB–Cur films. The tensile strength of pure PVB film and PVB–Cur film was 6 and 7.5 MPa, and the elongation at

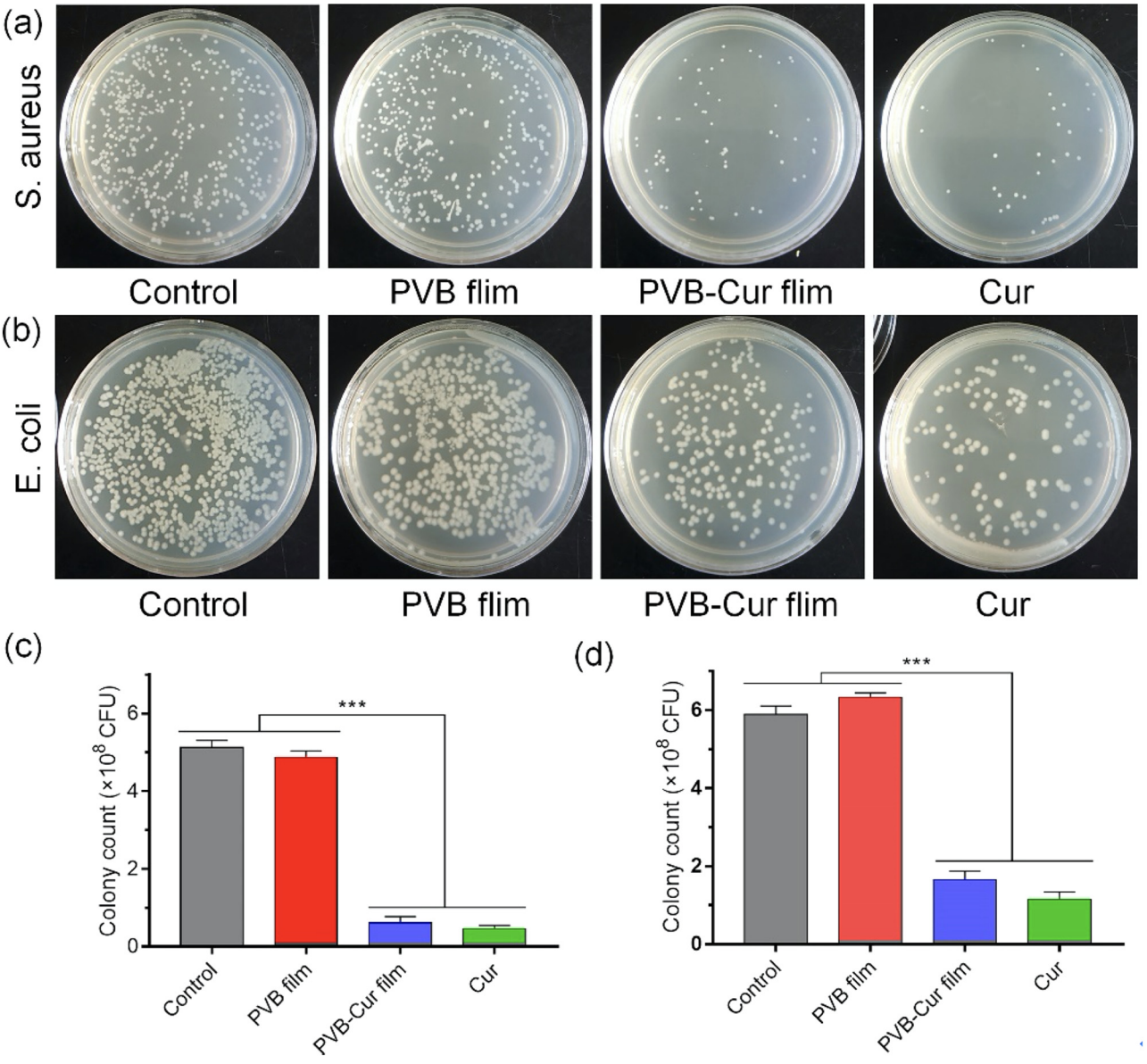

Figure 7: Antibacterial assays of *S. aureus* and *E. coli*. CFU photographs of *S. aureus* (a) and quantitative results (c). CFU photographs of *E. coli*. (b) and quantitative results (d).

break was 207% and 222%, respectively. The results demonstrated that the incorporation of Cur did not impair the mechanical properties of the films. The good mechanical properties of PVB–Cur composite films could be explained by a good interfacial interaction between Cur and PVB (20). It can be observed in Figure 5 that both PVB and PVB–Cur films exhibited yield behavior during tensile testing. This indicated that the film was not brittle, but an elastic plastic material. The stress–strain curves of PVB–Cur films exhibited elastic deformation regions with high modulus at the initial stage. The yield points were observed at approximately 3.5% strain. Subsequently, the strain-hardening region appeared in the stress–strain curve. At this stage, the enhancement in stress was accompanied by further elongation of the film. The excellent mechanical properties made the resulting films suitable candidates for food packaging (36).

3.5 Wettability property

The wettability of the film surfaces was investigated by measuring the water contact angle. Generally, when the angle between the water droplet and the surface of the film is less than 90° the surface of the film is judged to be hydrophilic, whereas the surface exceeding 90° is hydrophobic. Figure 6 shows the contact angle of the PVB film with and without Cur. Contact angle values at different times (0, 30, 60, 90, 120 s, respectively) were measured to analyze the time dependence. The starting contact angle of the PVB–Cur film was slightly lower than that of the PVB film. The starting contact angles of the PVB film and the PVB–Cur film were 78.1 ± 0.5° and 75.8 ± 0.6°, respectively. Therefore, both the PVB film and the PVB–Cur film were hydrophilic. Typically, the surface of the wound dressing with water contact angle of 60° to 80° could facilitate the adhesion and proliferation of cells at the wound (37). In addition, the contact angles of the PVB film and the PVB–Cur film were not constant, and there was a slight decrease of about 3° during the contact time of 0–60 s. After 60 s, the contact angle basically reached equilibrium. The incorporation of Cur slightly enhanced the hydrophilicity of the film, and the contact angle of the composite film could be maintained within the range that was favorable for wound healing.

3.6 Antibacterial activity

Bacterial proliferation is a key factor in causing food spoilage and wound infections. Therefore, the antibacterial property is very important for the application of film materials. Since *S. aureus* and *E. coli* are two common infectious species of bacteria in the natural environment, the activities of PVB–Cur film against these species were evaluated *in vitro*. The CFU quantification method was used to evaluate the antibacterial behavior of the materials. As shown in Figure 7, the PVB film did not exhibit noticeable antibacterial activity, compared to the Control group ($p > 0.05$). PVB–Cur film and Cur groups both possessed the ability to inhibit the growth of *S. aureus* and *E. coli* bacteria. The quantitative result of the colony count of *S. aureus* in the PVB–Cur film was $0.61 \pm 0.17 \times 10^8$, which was not different from that of the Cur group ($0.45 \pm 0.09 \times 10^8$), but significantly lower than those of the Control group and the PVB film group (***$p < 0.001$, one-way ANOVA with statistical software SPSS 14.0 (SPSS Inc., Chicago, USA)). The quantitative result of the colony count of *E. coli* in the PVB–Cur film was $1.65 \pm 0.22 \times 10^8$, which was also significantly lower than those of the Control group and the PVB film group (***$p < 0.001$). Therefore, the PVB–Cur film has robust antibacterial properties against both *S. aureus* and *E. coli*.

So far, the antibacterial mechanism of Cur has not been fully understood. Some studies had shown that the antibacterial effect of Cur was related to FtsZ, which was a cytoskeletal protein that plays an important role in the process of prokaryotic cell division. Here, Cur inhibited the growth of *E. coli* mainly by inhibiting the assembled FtsZ. In addition, Cur could damage bacterial membranes and improve their permeability. Cur is believed to have antibacterial properties by anchoring the cell wall of the bacterial cell, causing it to rupture and then infiltrating into the cell, destroying the structure of the organelle (38–40).

4 Conclusion

In this paper, PVB–Cur composite film was prepared using ethanol as the film-forming dispersions. FTIR spectroscopy analysis suggested that there were interactions between Cur and the PVB matrix. The UV-visible analysis indicated that the composite films exhibited better ultraviolet radiation-blocking properties than PVB films. Moreover, the addition of Cur improved the mechanical properties, hydrophilicity, and thermal properties of the PVB–Cur composite films. More importantly, the incorporation of Cur into the PVB matrix endowed the composite film with excellent antibacterial properties toward *E. coli*. Hence, the PVB–Cur composite film could be considered as potential candidate in the medical and food packaging industries.

Acknowledgment: This research was supported by a grant from the National Natural Science Foundation of China (NSFC) (No. 51703012).

References

(1) Liu C, Faria AF, Ma J, Elimelech M. Mitigation of biofilm development on thin-film composite membranes functionalized with zwitterionic polymers and silver nanoparticles. Environ Sci Technol. 2017;51:182–91.
(2) Yalcinkaya F, Lubasova D. Quantitative evaluation of antibacterial activities of nanoparticles (ZnO, TiO_2, ZnO/TiO_2, SnO_2, CuO, ZrO_2, and $AgNO_3$) incorporated into polyvinyl butyral nanofibers: quantitative evaluation of antibacterial activities of nanoparticles. Polym Adv Technol. 2017;28:137–40.
(3) Wei Q, Wang X, Cheng J-H, Zeng G, Sun D-W. Synthesis and antimicrobial activities of novel sorbic and benzoic acid amide derivatives. Food Chem. 2018;268:220–32.
(4) Yemenicioğlu A. Zein and its composites and blends with natural active compounds. Antimicrobial food packaging. Dordrecht, Netherlands: Elsevier; 2016. p. 503–13. ISBN 978-0-12-800723-5.
(5) Liu X, You L, Tarafder S, Zou L, Fang Z, Chen J, et al. Curcumin-releasing chitosan/aloe membrane for skin regeneration. Chem Eng J. 2019;359:1111–9.
(6) Cetin-Karaca H, Newman MC. Antimicrobial efficacy of plant phenolic compounds against *Salmonella* and *Escherichia Coli*. Food Biosci. 2015;11:8–16.
(7) Liu J, Liu S, Wu Q, Gu Y, Kan J, Jin C. Effect of protocatechuic acid incorporation on the physical, mechanical, structural and antioxidant properties of chitosan film. Food Hydrocoll. 2017;73:90–100.
(8) Bastarrachea L, Dhawan S, Sablani SS. Engineering properties of polymeric-based antimicrobial films for food packaging: a review. Food Eng Rev. 2011;3:79–93.
(9) Huang K-S, Yang C-H, Huang S-L, Chen C-Y, Lu Y-Y, Lin Y-S. Recent advances in antimicrobial polymers: a mini-review. Int J Mol Sci. 2016;17:1578.
(10) Wu C-S. Enhanced antibacterial activity, antioxidant, and *in vitro* biocompatibility of modified polycaprolactone-based membranes. Int J Polym Mater Polym Biomater. 2016;65:872–80.
(11) Mogoşanu GD, Grumezescu AM. Natural and synthetic polymers for wounds and burns dressing. Int J Pharm. 2014;463:127–36.
(12) Wang L, Xue J, Zhang Y. Preparation and characterization of curcumin loaded caseinate/zein nanocomposite film using pH-driven method. Ind Crops Prod. 2019;130:71–80.
(13) Ma Q, Cao L, Liang T, Li J, Lucia LA, Wang L. Active tara gum/PVA blend films with curcumin-loaded CTAC brush-TEMPO-oxidized cellulose nanocrystals. ACS Sustain Chem Eng. 2018;6:8926–34.
(14) Ma Q, Ren Y, Wang L. Investigation of antioxidant activity and release kinetics of curcumin from tara gum/polyvinyl alcohol active film. Food Hydrocoll. 2017;70:286–92.
(15) Akbik D, Ghadiri M, Chrzanowski W, Rohanizadeh R. Curcumin as a wound healing agent. Life Sci. 2014;116:1–7.
(16) Hussain Z, Thu HE, Amjad MW, Hussain F, Ahmed TA, Khan S. Exploring recent developments to improve antioxidant, anti-inflammatory and antimicrobial efficacy of curcumin: a review of new trends and future perspectives. Mater Sci Eng C. 2017;77:1316–26.
(17) Mohanty C, Sahoo SK. Curcumin and its topical formulations for wound healing applications. Drug Discovery Today. 2017;22:1582–92.
(18) Anand P, Kunnumakkara AB, Newman RA, Aggarwal BB. Bioavailability of curcumin: problems and promises. Mol Pharm. 2007;4:807–18.
(19) Liu Y, Cai Y, Jiang X, Wu J, Le X. Molecular interactions, characterization and antimicrobial activity of curcumin–chitosan blend films. Food Hydrocoll. 2016;52:564–72.
(20) Luo N, Varaprasad K, Reddy GVS, Rajulu AV, Zhang J. Preparation and characterization of cellulose/curcumin composite films. RSC Adv. 2012;2:8483.
(21) Govindaraj P, Kandasubramanian B, Kodam KM. Molecular interactions and antimicrobial activity of curcumin (*Curcuma longa*) loaded polyacrylonitrile films. Mater Chem Phys. 2014;147:934–41.
(22) Li X, Nan K, Li L, Zhang Z, Chen H. *In vivo* evaluation of curcumin nanoformulation loaded methoxy poly(ethylene glycol)-*graft*-chitosan composite film for wound healing application. Carbohydr Polym. 2012;88:84–90.
(23) Posavec D, Dorsch A, Bogner U, Bernhardt G, Nagl S. Polyvinyl butyral nanobeads: preparation, characterization, biocompatibility and cancer cell uptake. Microchim Acta. 2011;173:391–9.
(24) Liu G-S, Yan X, Yan F-F, Chen F-X, Hao L-Y, Chen S-J, et al. *In situ* electrospinning iodine-based fibrous meshes for antibacterial wound dressing. Nanoscale Res Lett. 2018;13:309.
(25) Chui C-Y, Mouthuy P-A, Ye H. Direct electrospinning of poly (vinyl butyral) onto human dermal fibroblasts using a portable device. Biotechnol Lett. 2018;40:737–44.
(26) Liu J, Wang H, Wang P, Guo M, Jiang S, Li X, et al. Films based on κ-carrageenan incorporated with curcumin for freshness monitoring. Food Hydrocoll. 2018;83:134–42.
(27) Wong S, Zhao J, Cao C, Wong CK, Kuchel RP, De Luca S, et al. Just add sugar for carbohydrate induced self-assembly of curcumin. Nat Commun. 2019;10:582.
(28) Pan J, Cao D, Ma X, Yang J. Preparation, characterization and in vitro release properties of pectin-based curcumin film. Korean J Chem Eng. 2019;36:822–7.
(29) Coscia MG, Bhardwaj J, Singh N, Santonicola MG, Richardson R, Thakur VK, et al. Manufacturing & characterization of regenerated cellulose/curcumin based sustainable composites fibers spun from environmentally benign solvents. Ind Crops Prod. 2018;111:536–43.
(30) Chen S, Chen X, Wu X. The mechanical behaviour of polyvinyl butyral at intermediate strain rates and different temperatures. Constr Build Mater. 2018;182:66–79.
(31) Xu S-C, Qin C-C, Yu M, Dong R-H, Yan X, Zhao H, et al. A battery-operated portable handheld electrospinning apparatus. Nanoscale. 2015;7:12351–5.
(32) Musso YS, Salgado PR, Mauri AN. Smart edible films based on gelatin and curcumin. Food Hydrocoll. 2017;66:8–15.
(33) Wang H, Hao L, Wang P, Chen M, Jiang S, Jiang S. Release kinetics and antibacterial activity of curcumin loaded zein fibers. Food Hydrocoll. 2017;63:437–46.

(34) Mohammadian-Kohol M, Nasrabadi MN, Navarchian AH, Jabbari I, Seyedhabashi MR. A study of the effects of gamma irradiation on the structural and mechanical properties of polyvinyl butyral film. Radiat Phys Chem. 2018;152:1–5.
(35) Ma Q, Du L, Wang L. Tara gum/polyvinyl alcohol-based colorimetric NH3 indicator films incorporating curcumin for intelligent packaging. Sens Actuators B. 2017;244:759–66.
(36) Haraguchi K, Ebato M, Takehisa T. Polymer–clay nanocomposites exhibiting abnormal necking phenomena accompanied by extremely large reversible elongations and excellent transparency. Adv Mater. 2006;18:2250–4.
(37) Mu X, Yu H, Zhang C, Chen X, Cheng Z, Bai R, et al. Nanoporous nitrocellulose liquid bandage modulates cell and cytokine response and accelerates cutaneous wound healing in a mouse model. Carbohydr Polym. 2016;136:618–29.
(38) Kaur S, Modi NH, Panda D, Roy N. Probing the binding site of curcumin in Escherichia coli and Bacillus subtilis FtsZ – A structural insight to unveil antibacterial activity of curcumin. Eur J Med Chem. 2010;45:4209–14.
(39) Tyagi P, Singh M, Kumari H, Kumari A, Mukhopadhyay K. Bactericidal activity of curcumin I is associated with damaging of bacterial membrane. PLoS One. 2015;10:1–15.
(40) Bhawana Basniwal RK, Buttar HS, Jain VK, Jain N. Curcumin nanoparticles: preparation, characterization, and antimicrobial study. J Agric Food Chem. 2011;59:2056–61.